Substitution Behavior and Stable Charge Carrier Species in Long-Bond Length Layered Cuprates

P. A. Salvador,[†,§] K. B. Greenwood,[‡] J. R. Mawdsley,[†] K. R. Poeppelmeier,*[,‡] and T. O. Mason[†]

Materials Science and Engineering Department, Northwestern University, 2225 N. Campus Dr., Evanston, Illinois 60208-3108, and Department of Chemistry, Northwestern University, 2145 Sheridan Rd., Evanston Illinois 60208

Received December 29, 1998. Revised Manuscript Received April 21, 1999

The stabilities of charge carriers, the transport properties, and the defect structures of the layered, quadruple perovskite $La_2Ba_2Cu_2Sn_2O_{11}$ have been investigated by chemical substitutions, powder X-ray diffraction, and simultaneous high-temperature electrical conductivity and thermopower measurements. The in-plane copper−oxygen bond lengths, in cooperation with the copper-coordination environment, are observed to control the chemical solubilities, stable charge carrier species, and oxygen defects. Potential n-type substitutions are successful via the substitution of niobium for tin. However, oxygen defects are demonstrated to be important compensation species for the incorporation of the substituted cations and in the mediation of the charge carrier concentration with the ambient atmosphere in the near-synthesis temperature region. These materials are intrinsic semiconductors and display crossover from n-type to p-type behavior with increasing oxygen partial pressure, from 10^{-5} to 1 atm pO_2, in the temperature range from 600 to 800 °C. Furthermore, the transport parameters are shown to be composition-dependent for these compounds and asymmetric with respect to electron and electron−hole conduction, in contrast to other layered copper oxides. Specifics of the inner architecture of layered copper oxides, particularly residual internal stresses between layers, are discussed with respect to their control over the redox behavior of copper−oxygen networks, and the implications of these findings are elaborated on with respect to the realization of new n-type superconductors.

1. Introduction

High-T_c superconductivity has been observed in many cuprate materials containing copper−oxygen layers of nominal stoichiometry CuO_2^{2-}. Although a variety of structural classes of layered cuprates support p-type high-T_c superconductivity (see refs 1−4), only two are believed to support n-type superconductivity.[5,6] This paucity of electron-doped superconducting cuprates remains poorly understood and evidences that the underlying electronic nature of, and the stability of carriers in, the superconducting layers of copper oxides warrant further research. This is further evidenced by the fact that several structural families exist, which adopt layered structures similar to the superconducting cuprates, that have not been observed to support superconductivity to date.[7−21] From both a chemical and physical perspective, the stability of the oxidation state

* Corresponding author.
† Materials Science and Engineering Department.
‡ Department of Chemistry.
§ Present address: Department of Materials Science and Engineering, Carnegie Mellon, University, 5000 Forbes Ave., Pittsburgh PA 15213-2890.

(1) Raveau, B.; Michel, C.; Hervieu, M.; Groult, D. *Crystal Chemistry of High-T_c Superconducting Copper Oxides*; Springer-Verlag: Berlin, 1991; Vol. 15, p 331.
(2) Raveau, B.; Michel, C.; Mercey, B.; Hamet, J. F.; Hervieu, M. *J. Alloys Compd.* **1995**, *229*, 134−143.
(3) Shaked, H.; Keane, P. M.; Rodriguez, J. C.; Owen, F. F.; Hitterman, R. L.; Jorgensen, J. D. *Crystal Structures of the High-T_c Superconducting Copper-Oxides*; Elsevier Science B.V.: Amsterdam, 1994.
(4) Salvador, P. A.; Mason, T. O.; Hagerman, M. E.; Poeppelmeier, K. R. In *Chemistry of Advanced Materials: An Overview*; Interrante, L. V., Hampden-Smith, M., Eds.; Wiley-VCH: New York, 1998; pp 449−498.
(5) Tokura, Y.; Takagi, H.; Uchida, S. *Nature* **1988**, *337*, 345−346.
(6) Smith, M. G.; Manthiram, A.; Zhou, J.; Goodenough, J. B.; Markert, J. T. *Nature* **1991**, *351*, 549−550.
(7) Murayama, N.; Sudo, E.; Kani, K.; Tsuzuki, A.; Kawakami, S.; Awano, M.; Torii, Y. *Jpn. J. Appl. Phys.* **1988**, *27*, L1623−L1625.
(8) Wiley, J. B.; Markham, L. M.; Vaughey, J. T.; McCarthy, T. J.; Sabat, M.; Hwu, S.-J.; Song, S. N.; Ketterson, J. B.; Poeppelmeier, K. R. In *Chemistry of High-Temperature Superconductors II*; Nelson, D. L., George, T. F., Eds.; American Chemical Society: Washington, DC, 1988; pp 304−314.
(9) Greaves, C.; Slater, P. R. *Physica C* **1989**, *161*, 245.
(10) Rey, M.-J.; Dehaudt, P.; Joubert, J.; Hewat, A. W. *Physica C* **1990**, *167*, 162−167.
(11) Wiley: J. B.; Sabat, M.; Hwu, S.-J.; Poeppelmeier, K. R. *J. Solid State Chem.* **1990**, *88*, 250−260.
(12) Vaughey, J. T.; Shumaker, R.; Song, S. N.; Ketterson, J. B.; Poeppelmeier, K. R. *Mol. Cryst. Liq. Cryst.* **1990**, *184*, 335−342.
(13) Vaughey, J. T.; Wiley, J. B.; Poeppelmeier, K. R. *Z. Anorg. Allg. Chem.* **1991**, *598/599*, 327−338.
(14) Anderson, M. T.; Poeppelmeier, K. R. *Chem. Mater.* **1991**, *3*, 476−482.
(15) Anderson, M. T.; Poeppelmeier, K. R.; Zhang, J. P.; Fan, H.-J.; Marks, L. D. *Chem. Mater.* **1992**, *4*, 1305−1313.
(16) Gormezano, A.; Weller, M. T. *J. Mater. Chem.* **1993**, *3*, 979−982.
(17) Gormezano, A.; Weller, M. T. *J. Mater. Chem.* **1993**, *3*, 771−772.
(18) Greenwood, K. B.; Anderson, M. T.; Poeppelmeier, K. R.; Novikov, D. L.; Freeman, A. J.; Dabrowski, B.; Gramsch, S. A.; Burdett, J. K. *Physica C* **1994**, *235−240*, 349−350.
(19) Zhu, W. J.; Huang, Y. Z.; Ning, T. S.; Zhao, Z. X. *Mater. Res. Bull.* **1995**, *30*, 243−246.

10.1021/cm9811489 CCC: $18.00
Published on Web 06/04/1999

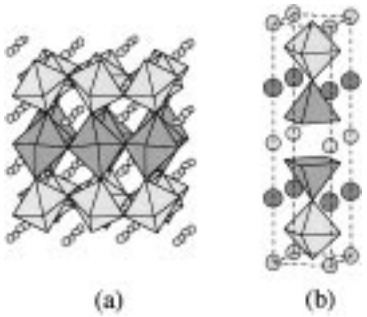

Figure 1. Structures of the layered copper−tin perovskite oxides (a) La_2CuSnO_6 and (b) $La_2Ba_2Cu_2Sn_2O_{11}$. In a, tin resides at the center of the light octahedra, copper resides at the center of the dark octahedra, and the light spheres represent lanthanum cations. In b, tin resides at the center of the light octahedra, copper at the center of the dark square pyramids, barium preferentially resides on the sites between the dissimilar polyhedra, represented by dark spheres, and lanthanum preferentially resides on the sites, denoted by light spheres.

of the copper−oxygen network, $CuO_2^{(2\pm\delta)}$, represents a fundamental concern not only for realizing new superconducting materials but also for optimizing existing cuprate superconductors and for understanding the nature of the electronic states of these (and other) transition metal oxides.

To develop further our understanding of the chemical factors which control these technologically important properties, we have investigated structurally layered cuprates and the relationships between their defect structures and physicochemical properties, with an emphasis on the preeminent relationship between the internal chemistry and inner architecture (see refs 4 and 22). Two materials which are of interest as potential n-type superconductors are La_2CuSnO_6[14] and $La_2Ba_2Cu_2Sn_2O_{11}$,[15] whose structures are depicted in Figure 1, parts a and b, respectively. Both compounds are built up of alternating perovskite blocks having either copper or tin as the framework *B*-cation. In the former compound, an oxygen-stoichiometric double perovskite, octahedral copper cations alternate with octahedral tin cations along the (001) direction of the unit cell, thereby creating single CuO_2^{2-} and SnO_2^0 layers. The copper coordination can be, at first glance, likened to that in La_2CuO_4 or Ba_2CuHgO_4, in that single layers of corner-sharing octahedral copper−oxygen polyhedra are essential structural features.

In $La_2Ba_2Cu_2Sn_2O_{11}$,[15] as depicted in Figure 1b, oxygen-deficient, copper-based, perovskite bilayers alternate with oxygen-stoichiometric, tin-based, perovskite bilayers along the (001) axis of the unit cell. This motif creates a coordination environment in the copper-based layers similar to that observed in the $REBa_2Cu_3O_{7-\delta}$,[23,24] $GaRESr_2Cu_2O_7$,[25] and $La_2AECu_2O_{6\pm x}$[26] superconducting materials (*RE* = rare earth, *AE* = alkaline earth). The interleaving tin-based perovskite layers stabilize long, in-plane bond lengths, ∼2 Å, yet the high-temperature transport properties were demonstrated to be similar to the p-type layered-cuprate superconductors in the undoped state.[27]

While both of these compounds have structural features reminiscent of the high-temperature superconductors, neither has been shown to superconduct. Even when strontium or calcium substitutes for lanthanum in La_2CuSnO_6, the phase remains nonsuperconducting.[14,28−30] As shown in Figure 1a, the CuO_2^{2-} and SnO_2^0 layers are severely buckled and the average in-plane Cu−O bond length is nearly 2 Å, which is too large for hole-doped superconductors. It has also been shown that, when doped with holes, the in-plane bond lengths increased and the out-of-plane bond lengths decreased. This has been attributed to the increased importance of the d_{z^2} orbital near the Fermi level, as compared to the $d_{x^2-y^2}$ orbital in other layered cuprates, owing to the specifics of the local copper coordination. It is expected that the removal of an apical copper−oxygen interaction will lower the energy of the d_{z^2} orbital to which it is associated, with respect to its position in La_2CuSnO_6, and place the $d_{x^2-y^2}$ orbital nearer to the Fermi level for $La_2Ba_2Cu_2Sn_2O_{11}$. This should lead to electrical properties more similar to the "electronically"-layered cuprates, as were observed for the undoped compound.[30]

While the structural features and some of the physical properties of these compounds have been reported previously,[14,15,27−30] this paper reports on the relationship between the internal chemistry and the stability of carriers in these materials with respect to the electronic states of copper owing to the specifics of the inner architecture of these unique materials. The in-plane copper−oxygen bond lengths of 2 Å for both copper−stannate families are much greater than those observed in the p-type layered cuprates. Moreover, these values are larger than those in both of the n-type cuprate superconductors, $Sr_{1-x}Nd_xCuO_2$[6] and $Nd_{2-x}Ce_xCuO_4$,[5] which have bond lengths near 1.97 Å. Long, in-plane bond lengths have been attributed to the stabilization of electron doping (a reduction of the overall charge on the $CuO_2^{(2\pm\delta)-}$ layers) in cuprates. However, this has not led to an extensive understanding of the absence of stable electron-doped materials in compounds having bond lengths longer than 1.97 Å. Moreover, we have found that hole-type carriers are stable in the triple and quadruple perovskites with bond lengths

(20) Otzschi, K. D.; Poeppelmeier, K. R.; Salvador, P. A.; Mason, T. O.; Zhang, H.; Marks, L. D. *J. Am. Chem. Soc.* **1996**, *118*, 8951−8952.
(21) Otzschi, K. D.; Poeppelmeier, K. R.; Salvador, P. A.; Mason, T. O.; Sinkler, W.; Zhang, H.; Marks, L. D. *Physica C* **1997**, *282−287*, 837−838.
(22) Salvador, P. A.; Mason, T. O.; Otzschi, K.; Greenwood, K. B.; Poeppelmeier, K. R.; Dabrowski, B. *J. Am. Chem. Soc.* **1997**, *119*, 3756−3764.
(23) Wu, M. K.; Ashburn, J. R.; Torng, C. J.; Hor, P. H.; Meng, R. L.; Gao, L.; Huang, Z. J.; Wang, Y. Q.; Chu, C. W. *Phys. Rev. Lett.* **1987**, *58*, 908−910.
(24) Beno, M. A.; Soderholm, L.; Capone, D. W., II; Hinks, D. G.; Jorgensen, J. D.; Grace, J. D.; Schuller, I. K.; Segre, C. U.; Zhang, K. *Appl. Phys. Lett.* **1987**, *51*, 57−59.
(25) Vaughey, J. T.; Thiel, J. P.; Hasty, E. F.; Groenke, D. A.; Stern, C. L.; Poeppelmeier, K. R.; Dabrowski, B.; Hinks, D. G.; Mitchell, A. W. *Chem. Mater.* **1991**, *3*, 935−940.
(26) Nguyen, N.; Er-Rakho, L.; Michel, C.; Choisnet, J.; Raveau, B. *Mater. Res. Bull.* **1980**, *15*, 891−897.
(27) Salvador, P. A.; Shen, L.; Mason, T. O.; Greenwood, K. B.; Poeppelmeier, K. R. *J. Solid State Chem.* **1995**, *119*, 80−89.
(28) Anderson, M. T.; Poeppelmeier, K. R.; Gramsch, S. A.; Burdett, J. K. *J. Solid State Chem.* **1993**, *102*, 164−174.
(29) Novikov, D. L.; Freeman, A. J.; Poeppelmeier, K. R.; Zhukov, V. P. *Physica C* **1995**, *252*, 7−12.
(30) Salvador, P. A.; Otzschi, K.; Zhang, H.; Mawdsley, J. R.; Greenwood, K. B.; Dabrowski, B. M.; Marks, L. D.; Mason, T. O.; Poeppelmeier, K. R. In *Solid State Chemistry of Inorganic Materials*; Davies, P. K., Jacobson, Torardi, A. J. C. C., Vanderah, T. A., Eds.; Materials Research Society: Pittsburgh, PA, 1997; Vol. 453; pp 311−322.

greater than 1.97 Å, i.e., $LaBa_2Cu_2NbO_8$ and $La_2Ba_2Cu_2Ti_2O_{11}$.[22,31] These results are a clear indication that other aspects of the inner architecture of these complex oxides feature prominently in the stabilization of charge carriers.

Herein, we report the high-temperature transport properties and defect structure of compounds in the $La_2Ba_2Cu_2Sn_{2-x}Nb_xO_{11}$ ($x \leq 0.2$) series. This series is compared to the $La_{2-x}Sr_xCuSn_{1-y}Nb_yO_6$ series (herein and ref 30), and various related layered cuprates in order to understand the stability of charge carriers in complex copper oxides. The stability of charge carriers is discussed in the context of bond mismatch between layers, first presented by Goodenough and Manthiram,[32] with the additional effects of copper coordination and orbital competition included. The possibility of realizing new n-type compounds within this framework is presented.

2. Experimental Section

Samples were prepared by the solid-state reaction of stoichiometric amounts of barium carbonate (Aldrich, 99.999%), strontium carbonate (Aldrich, 99.999%), copper(II) oxide (Aldrich, 99.99+%), tin(IV) oxide (Aldrich, 99.995+%), lanthanum oxide (Aldrich, 99.999%), and niobium oxide (Aldrich, 99.99%). The reagents were intimately ground and then fired in high-density alumina boats at 950 °C in air for 1 day. Each sample was air quenched, reground, and pressed into two pellets; one that was less than 1 mm thick and another that was several millimeters thick. The pellets were then fired between 1010 and 1050 °C in air. The thin pellet was employed as a barrier to prevent diffusion of aluminum into the sample, while the large pellet was quenched, ground and fired several times during the course of a seven-day reaction period.

A Rigaku diffractometer with nickel-filtered Cu Kα radiation was employed to collect diffraction data on the quenched polycrystalline samples. Phase purity of the samples was ensured by collecting data with a 2θ scan from 15 to 90° with a step of 0.02° and a collection time of 10 s at each step. Lattice parameters were determined using Rietveld analysis[33] on the diffraction data, using previously reported structural models.[14,15]

Simultaneous four-point conductivity and thermoelectric coefficient measurements, at temperatures ranging from 650 to 820 °C, were carried out on the single-phase samples, using an apparatus described previously.[34] The measured conductivities were corrected to account for the relative density of the specimens (70−85%).[35] Flowing premixtures of oxygen and argon were used to vary the oxygen partial pressure above the sample, from 10^{-5} to 1 atm of oxygen, while the total pressure was maintained at one atmosphere. A Thermox (Pittsburgh, PA) oxygen meter, placed downstream from the sample, was used to confirm the oxygen partial pressure. Measurements were taken only after steady state had been achieved; typical equilibration times were 8−12 h per datum.

3. Results and Analysis

3.1. Solid Solution and Thermogravimetric Results. Powder X-ray diffraction (XRD) indicated that single-phase samples (with respect to the XRD sensitivity) were obtained for the following stoichiometry ranges: $La_2Ba_2Cu_2Sn_{2-x}Nb_xO_{11\pm\delta}$ ($0.0 \leq x \leq 0.2$) and $La_{2-x}Sr_xCuSn_{1-y}Nb_yO_6$ ($0.0 < x \leq 0.15$, $y = 0$). Significant amounts of impurity phases were observed for stoichiometries outside these ranges. Diffraction patterns of samples from the $La_2CuSn_{1-x}Nb_xO_6$ series displayed both impurity phases and extremely broad diffraction peaks, indicating that the products were poorly reacted and multiphase even after prolonged heating at elevated temperatures. Thus, these materials were not further characterized. The ability of niobium to substitute for tin in the quadruple perovskite but not in the double perovskite is associated with available compensation mechanisms and will be elaborated on further below.

The lattice parameters (space group $P4/mmm$) of select samples in the $La_2Ba_2Cu_2Sn_{2-x}Nb_xO_{11\pm\delta}$ series are as follows: $x = 0.0$, $a = 3.9893(3)$, $c = 16.232(1)$; $x = 0.15$, $a = 3.9871(1)$, $c = 16.200(1)$; $x = 0.20$, $a = 3.9886(1)$, $c = 16.198(1)$. The values for the doped compounds show a small decrease in both a and c with increased doping level, but it appears the lattice parameters are not changing much between $x = 0.15$ and $x = 0.20$. This could indicate that either the solubility limit is between these two values, despite the absence of impurity phases in the XRD patterns, or that the compensation mechanism for the substitution of niobium atoms does not lead to a straightforward variation in the lattice parameters with dopant level. While one might expect Vegard's Law to be obeyed by these substituted quadruple perovskites (and the isostructural materials $Ln_2Ba_2Cu_2Ti_2O_{11}$, Ln = lanthanide, Y), resulting in linear variations of the cell parameters vs doping, depending on the relative size of the substituted cation to the host cation, this simple behavior is not observed in these systems.[36] In the $La_2Ba_2Cu_2Sn_{2-x}Nb_xO_{11\pm\delta}$ compounds, atomic displacements (rotations of the tin/niobium octahedra), electronic carriers, and oxygen defects are introduced concomitantly with the addition of niobium, thereby leading to a more complex relationship between doping level and lattice parameters.

No conditions could be found where the oxygen content could be accurately determined from the endpoints of thermogravimetric experiments in the $La_2Ba_2Cu_2Sn_{2-x}Nb_xO_{11\pm\delta}$ system. This resulted from the fact that the niobium oxidation state could not be accurately ascertained in the presence of the complex mix of cations (also Nb_2O_5 was observed to reduce under the working conditions). The electrical property measurements were therefore used to estimate the overall oxygen contents, with respect to their effect on the average oxidation state in the CuO_2^{2-} planes (i.e., the number of carriers).

3.2. Electrical Properties and Jonker Analysis. The high-temperature electrical properties for the samples $La_2Ba_2Cu_2Sn_2O_{11\pm\delta}$ (data taken from ref 27), $La_2Ba_2Cu_2Sn_{1.90}Nb_{0.10}O_{11\pm\delta}$, $La_2Ba_2Cu_2Sn_{1.85}Nb_{0.15}O_{11\pm\delta}$, and $La_2Ba_2Cu_2Sn_{1.80}Nb_{0.20}O_{11\pm\delta}$ are given in Figures 2−5, respectively, and are presented in the form of

(31) Salvador, P. A.; Greenwood, K. B.; Otzschi, K.; Koentizer, J. W.; Dabrowski, B. M.; Poeppelmeier, K. R.; Mason, T. O. In *Solid-State Chemistry of Inorganic Materials*; Davies, P. K., Jacobson, A. J., Torardi, C. C., Vanderah, T. A., Eds.; Materials Research Society: Pittsburgh, PA, 1997; Vol. 453; pp 171−176.

(32) Goodenough, J. B.; Manthiram, A. *J. Solid State Chem.* **1990**, *88*, 115−139.

(33) Wiles, D. B.; Sakthivel, A.; Young, R. A. *Rietveld Analysis Program DBWS-9006PC*; School of Physics, Georgia Institute of Technology; Atlanta, GA, 1990.

(34) Trestman-Matts, A.; Dorris, S. E.; Mason, T. O. *J. Am. Ceram. Soc.* **1983**, *66*, 589−591.

(35) McLachlan, D. S.; Blaszkiewicz, M.; Newnham, R. E. *J. Am. Ceram. Soc.* **1990**, *73*, 2187−2203.

(36) Greenwood, K. B. Ph.D. Thesis, Northwestern University, 1995.

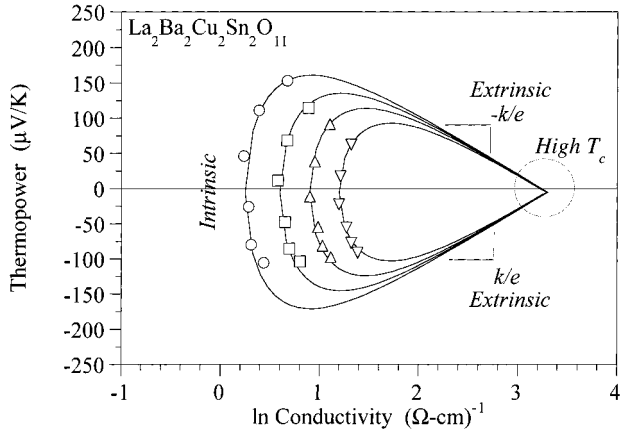

Figure 2. Jonker analysis of the thermopower and conductivity data (taken from ref 27) for $La_2Ba_2Cu_2Sn_2O_{11\pm\delta}$ at the following four temperatures: ○ = 650 °C, □ = 705 °C, △ = 765 °C, and ▽ = 820 °C. Data at each temperature correspond to oxygen partial pressures of 10^0, 10^{-1}, 10^{-2}, 10^{-3}, 10^{-4}, and 10^{-5} in a counterclockwise fashion. See text for explanation of the demarcations of the distinct regimes on the Jonker curves.

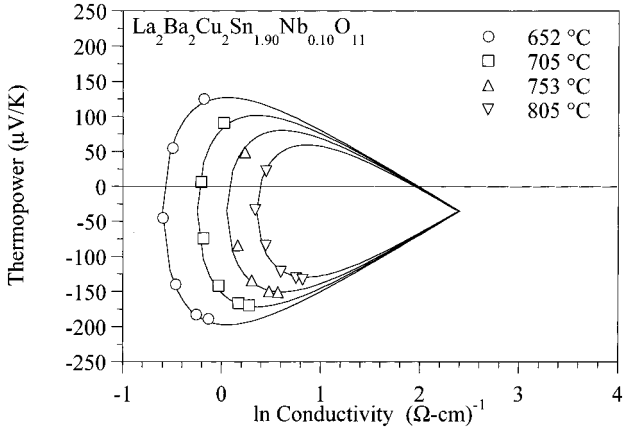

Figure 3. Jonker analysis of the thermopower and conductivity data for $La_2Ba_2Cu_2Sn_{1.90}Nb_{0.10}O_{11\pm\delta}$ at four temperatures. Data at each temperature correspond to oxygen partial pressures of 10^0, 10^{-1}, 10^{-2}, 10^{-3}, 10^{-4}, and 10^{-5} in a counterclockwise fashion.

Jonker plots (after ref 37). In Jonker plots, the thermopower is plotted as a function of the natural logarithm of the conductivity, and the solid curves in Figures 2−5 are fits to these data using the two-band semiconductor model, as developed by Jonker[37] and discussed further below. The usefulness of this analysis method for elucidating the transport properties and the internal chemistry of semiconducting and superconducting cuprates, as well as its underlying mathematical basis, have been discussed in detail elsewhere.[22,27,37,38] However, some of the mathematical basis of these curves will be discussed below with respect to locating the intrinsic composition.

Several qualitative aspects of Jonker analysis are of particular importance with respect to the internal chemistry of these materials, such as the region of the curve on which the data lie and also the spread of the data as a function of both the oxygen partial pressure

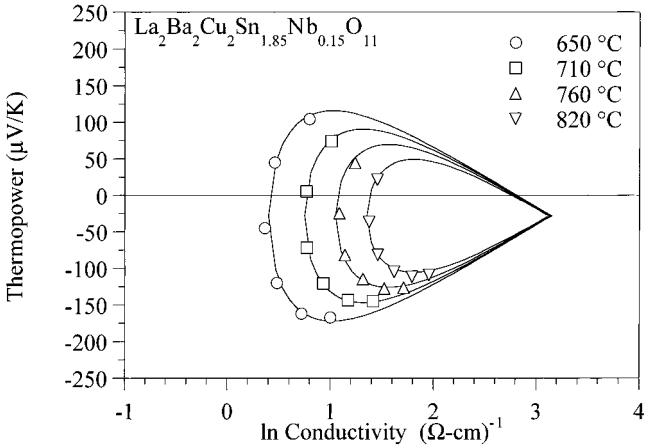

Figure 4. Jonker analysis of the thermopower and conductivity data for $La_2Ba_2Cu_2Sn_{1.85}Nb_{0.15}O_{11\pm\delta}$ at four temperatures. Data at each temperature correspond to oxygen partial pressures of 10^0, 10^{-1}, 10^{-2}, 10^{-3}, 10^{-4}, and 10^{-5} in a counterclockwise fashion.

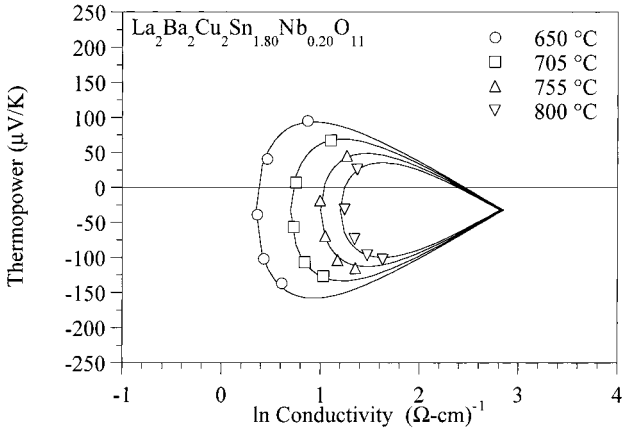

Figure 5. Jonker analysis of the thermopower and conductivity data for $La_2Ba_2Cu_2Sn_{1.80}Nb_{0.20}O_{11\pm\delta}$ at four temperatures. Data at each temperature correspond to oxygen partial pressures of 10^0, 10^{-1}, 10^{-2}, 10^{-3}, and 10^{-4} in a counterclockwise fashion.

and chemical composition. The characteristic "pear"-shape of the fitted curves (see below) is evident in Figures 2−5. The region of the curve on which the data lie is an indication of the type and amount of charge carriers in layered cuprates.[22,27,31,38] For instance the data for $La_2Ba_2Cu_2Sn_2O_{11}$, given in Figure 2, all lie on the region of the curve on the low-conductivity side of the thermopower maxima, which corresponds to the intrinsic regime where two types of carriers (electrons and holes) contribute to the electrical properties. The extrinsic regimes are marked in Figure 2 along with their characteristic slopes; $-k/e$ for p-type semiconductors (positive thermopower values) and $+k/e$ for n-type semiconductors (negative thermopower values). Also denoted in Figure 2 is the regime where data for high-T_c superconducting cuprates fall (usually below a thermopower of ± 40 μV/K). This region corresponds to a heavily doped material, which may either be a degenerate semiconductor or metal, and the data may deviate strongly from the curves based on two-band semiconductor theory, owing to the change in the conduction process.

It is evident in Figures 2−5, that the gross qualitative features of the Jonker plots for all four compounds are

(37) Jonker, G. H. *Philips Res. Rep.* **1968**, *23*, 131−138.
(38) Su, M.-Y.; Elsbernd, C. E.; Mason, T. O. *J. Am. Ceram. Soc.* **1990**, *73*, 415−419.

similar. A predominance of data in the two-carrier conduction regime (the intrinsic regime) and a strong dependence of the electrical properties on the oxygen partial pressure are observed. In each figure, the data at any particular temperature corresponds to log pO_2 values of 0, −1, −2, −3, −4, and −5 starting from the most positive thermopower values, where log $pO_2 = 0$, and continuing in order of decreasing pO_2 in a counterclockwise fashion around the curve. Transitions from positive to negative thermopower values are observed for all four compounds as a function of oxygen partial pressure. Thermal generation of carriers is responsible for the increase in the conductivity minimum as temperature is increased for all of the materials. The maximum conductivity can be modeled fairly well as a fixed value for each sample, as observed for other layered cuprates, and this is consistent with itinerant carriers or polaronic carriers with activation energies on the order of kT.[37,39]

Importantly, niobium substitution does not lead to the appropriate electronic state required for high-temperature superconductivity. The qualitative equivalence of both the position of the data and their behavior with respect to variation in the oxygen partial pressure indicates that despite the successful substitution of niobium for tin in these compounds, electronic compensation is not the predominant compensation mechanism. Oxygen defects, most likely similar to those in the parent compound and related phases,[22,27] are controlling the oxidation state of the copper−oxygen planes in these materials. Despite this similarity, there is some indication that at low-oxygen partial pressures, the niobium-substituted materials exhibit electron dominated conductivity and are beginning to transition into the extrinsic regime. It is evident, however, that these compositions cannot be driven to superconductivity simply by chemical substitution, and these data suggest that further reducing anneals would be required to reach the appropriate electronic state. However, decomposition of the materials was observed for reducing anneals in argon at the synthesis temperature.

More subtle changes in the electronic properties can be observed if we consider the quantitative features of the Jonker curves. The size and shape of the Jonker "pear" depend only on the intrinsic material parameters as follows:

$$\ln\left(\frac{2\sigma_{max}}{\sigma_{min}}\right) = \left(\frac{E_G}{2kT} + \frac{A_+ + A_-}{2}\right) \quad (1)$$

where σ_{min} is the minimum conductivity, σ_{max} is the maximum conductivity, E_G is the band gap, k is Boltzman's constant, T is the temperature, and A_+ and A_- are the transport coefficients for electron−holes and electrons, respectively.[37,38] The axis of symmetry of the resulting curves may lie at a nonzero value along the thermopower axis. This offset is a result of an asymmetry in the conduction parameters for electrons and holes, and is given by

$$Q_{off} = \frac{k}{2e}\ln\frac{N_+ e^{A_+}\mu_+}{N_- e^{A_-}\mu_-} \quad (2)$$

where, e is the unit of electronic charge, and N, A, and μ are the density of states, transport coefficient, and mobility of carriers, respectively, the type of which is denoted by the appropriate subscript (+ for holes and − for electrons).[37] The overall asymmetry, or the ratio inside the logarithmic term on the right-hand side of eq 2, can be determined by the fitting of Q_{off}. It should be noted that when the conduction parameters are symmetric with respect to the different carriers then this ratio is unity, the minimum conductivity value corresponds to the intrinsic conductivity and the axis of symmetry is along the zero thermopower axis. This is the case for the majority of layered cuprates investigated in similar temperature regimes. Furthermore, it can be shown that if the mobilities of the two carriers are equal, then the intrinsic composition (n = p) has a thermopower value corresponding to the offset thermopower value and a conductivity value corresponding to the conductivity minimum; in other words the intrinsic composition is along the axis of symmetry of the Jonker pear. However, if the asymmetry arises from differences in mobilities, then the thermopower value of the intrinsic composition, Q_i, can be shown to be equal to

$$Q_i = \frac{-k}{e}\left(\frac{1-a}{1+a}\right)\ln\left(\frac{2\sigma_{max}}{\sigma_{min}}\right) \quad (3)$$

wherein

$$a = e^{(2kQ_{off}/e)} \quad (4)$$

Table 1. Jonker Fit Parameters and Intrinsic Gap Energies from High-Temperature Electrical Data of $La_2Ba_2Cu_2Sn_2O_{11}$, $La_2Ba_2Cu_2Sn_{1.90}Nb_{0.10}O_{11}$, $La_2Ba_2Cu_2Sn_{1.85}Nb_{0.15}O_{11}$, and $La_2Ba_2Cu_2Sn_{1.80}Nb_{0.20}O_{11}$

			E_G (eV)		
T (K)	ln σ_{min}	ln σ_{max}	band ($A = 2$)	small polaron ($A = 0$)	Q_i (μV/K) (if $\mu_+ < \mu_-$)
			$La_2Ba_2Cu_2Sn_2O_{11\pm\delta}$[a,b]		
923	0.25	3.3	0.28	0.6	−19
978	0.60	3.3	0.23	0.57	−17
1038	0.90	3.3	0.20	0.55	−15
1093	1.20	3.3	0.15	0.53	−14
			$La_2Ba_2Cu_2Sn_{1.90}Nb_{0.10}O_{11\pm\delta}$[c]		
923	−0.6	2.4	0.27	0.59	−123
983	−0.25	2.4	0.23	0.56	−111
1038	0.05	2.4	0.18	0.54	−101
1093	0.35	2.4	0.14	0.51	−91
			$La_2Ba_2Cu_2Sn_{1.85}Nb_{0.15}O_{11\pm\delta}$[d]		
923	0.4	3.15	0.23	0.55	−93
983	0.75	3.15	0.19	0.52	−84
1038	1.05	3.15	0.14	0.50	−76
1093	1.35	3.15	0.09	0.47	−67
			$La_2Ba_2Cu_2Sn_{1.80}Nb_{0.20}O_{11\pm\delta}$[e]		
923	0.35	2.85	0.19	0.51	−98
978	0.70	2.85	0.14	0.48	−87
1028	1.0	2.85	0.09	0.45	−78
1073	1.2	2.85	0.06	0.43	−72

[a] Data taken from ref 27. [b] $Q_{off} = -5$, transport asymmetry is = 1/1.12. [c] $Q_{off} = -35$, transport asymmetry is = 1/2.25. [d] $Q_{off} = -28$, transport asymmetry is = 1/1.92. [e] $Q_{off} = -32$, transport asymmetry is = 1/2.10.

The fit parameters to the data displayed in Figures 2−5 are given in Table 1 and include the minimum and

(39) Hong, B. S.; Mason, T. O. *Solid State Ionics* **1991**, *49*, 3−7.

maximum conductivity, and the offset of the axis of symmetry from the zero thermopower axis (which corresponds to the intrinsic value if the mobilities of the two carriers are equal). These determined values suggest that the transport product, $Ne^A\mu$, for electrons is about 2 times larger than that for holes in the niobium-doped stannate materials. It is interesting to note that no other layered cuprates have been modeled with such different transport products, but the majority have been modeled with symmetric transport parameters (i.e., equal transport products for electrons and holes).[31,38] Also given in Table 1 are the effective band gaps for the cases where the transport occurs via itinerant carriers or small polarons, where A is 2 and 0, respectively.[40] Finally, the intrinsic thermopower values are given in Table 1 for the case where the asymmetry arises from inequivalent mobilities for the two carriers (these were calculated in accordance with eqs 1−4 using the fit parameters given in Table 1). The values of Q_i (for the case where $\mu_+ \neq \mu_-$), are given as an extreme indication as to where the intrinsic (n = p) composition may lie along the curves, and not to imply that the asymmetry definitely arises from mobility differences. Further experiments are necessary to determine which parameter (or parameters) in the transport product leads to the observed asymmetry, but the implications of this asymmetry and possible origins will be discussed below.

The band gap values for the copper−tin quadruple perovskites, see Table 1, are quite small, both with respect to kT at the measurement temperatures and to those of other layered cuprates.[27,38,41,42] Niobium-substituted materials not only have an asymmetry in the transport parameters but also have decreased effective band gap energies. This decrease has important ramifications for the defect analysis and for doping compensation and can be related to the crystal chemistry of the copper−oxygen network, as discussed below. It is important to note that the effective band gap, for band semiconductivity ($A = 2$) yields results which are on the order of kT. Classical Jonker analysis, which relies on Boltzman's statistics for its validity, breaks down in this region, owing to the highly degenerate nature of the semiconductor.[37] However, analytical expressions which use Fermi integrals, in the place of Boltzman's approximations, can be used to generate similarly shaped plots. Therefore, the band gap values can only be viewed as approximations to the values obtained using the more accurate analytical expressions. Fortunately, the overall shape of the Jonker pear is retained in the highly degenerate intrinsic region, and this leads to the excellent empirical fits seen in Figures 2−5.

3.3. Defect Chemistry/Compensation Mechanisms. It is difficult to completely solve the defect structure of these complex materials without more precise oxygen content determinations or further structural investigations having more sensitivity with respect to oxygen anions. However, from the current data we

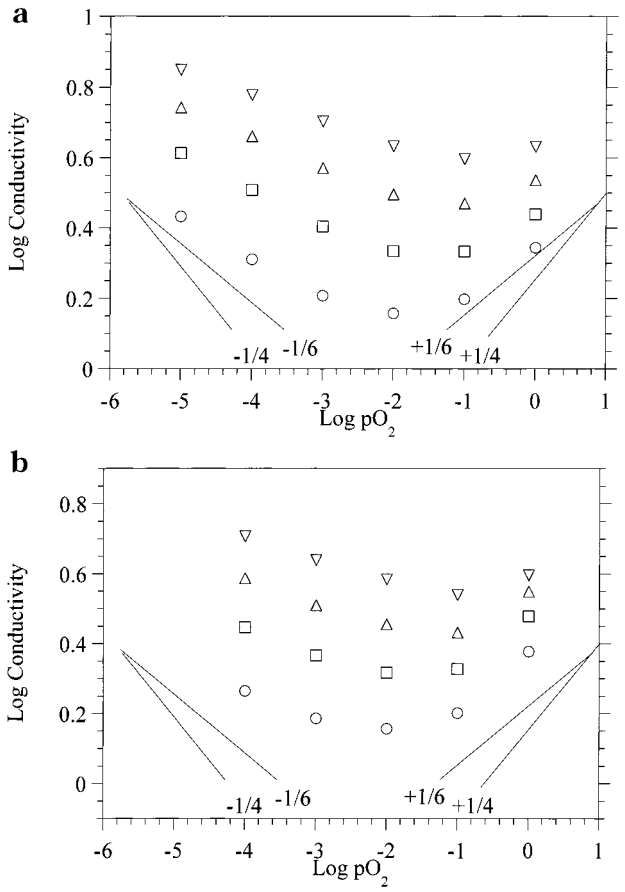

Figure 6. Logarithm of conductivity versus the logarithm of oxygen partial pressure (Brouwer plot) for (a) $La_2Ba_2Cu_2Sn_{1.85}Nb_{0.15}O_{11\pm\delta}$ and (b) $La_2Ba_2Cu_2Sn_{1.80}Nb_{0.20}O_{11\pm\delta}$. The classical defect slopes ($\pm^1/_6$ and $\pm^1/_4$) are given as guides to the eye.

can make some firm assertions concerning the general defect structure. A key feature of the electrical properties is the existence of dual carrier transport over the entire ranges of substitutions, oxygen pressures, and temperatures, for the $La_2Ba_2Cu_2Sn_{2-x}Nb_xO_{11\pm\delta}$ series. This rules out electronic compensation as the mechanism which counterbalances the increase in positive charge as a result of niobium substitution on tin sites: if this were not the case we would expect highly doped materials having a rather low negative thermopower values, but on the extrinsic leg of the pair. Nearly the entire range of intrinsic electrical properties is traversed over the experimental range of oxygen partial pressures. Because of this transitional behavior, and the degenerate electronic state of these small band gap semiconductors, slopes indicative of particular defect mechanisms are not observed in log conductivity vs log oxygen partial pressure plots. Parts a and b of Figure 6 are two such plots, for $La_2Ba_2Cu_2Sn_{1.85}Nb_{0.15}O_{11\pm\delta}$ and $La_2Ba_2Cu_2Sn_{1.80}Nb_{0.20}O_{11\pm\delta}$, respectively; these plots are similar to that for $La_2Ba_2Cu_2Sn_2O_{11}$.[27] Slopes of $\pm^1/_6$ and $\pm^1/_4$ (standard slopes for doubly ionized oxygen defects depending on the overall electroneutrality conditions—see refs 43−47) are given in these plots as a guide to

(40) Ioffe, A. F. *Physics of Semiconductors*; Infosearch Limited: London, 1960.
(41) Su, M.-Y.; Elsbernd, C. E.; Mason, T. O. *Physica C* **1989**, *160*, 114−118.
(42) Shen, L.; Salvador, P. A.; Mason, T. O. *J. Phys. Chem. Solids* **1996**, *57*, 1311−1319.
(43) Brouwer, G. *Philips Res. Rep.* **1954**, *9*, 366−376.
(44) Kröger, F. A.; Vink, H. J. In *Solid State Physics: Advances in Research and Applications*; Seitz, F., Turnbull, D., Eds.; Academic Press Inc.: New York, 1956; Vol. 3, pp 307−435.
(45) Kröger, F. A.; Stieltjes, F. H.; Vink, H. J. *Philips Res. Rep.* **1959**, *14*, 557−601.

the eye. It is apparent that the experimental slopes are nonzero, yet much shallower than the classical defect slopes, indicating that the transitional behavior and the narrow extent of the "intrinsic" region with respect to oxygen partial pressure precludes determination of the majority defect species.

Owing to the predominance of dual carrier transport behavior, the nominal stoichiometries requiring excess negative charge with respect to the parent structure, and the structural relationship to other materials in which interstitial oxygen are observed, we can speculate that the niobium cations are compensated by interstitial oxygen, according to the following electroneutrality condition, using Kröger and Vink notation:[44,45]

$$[Nb_{Sn}^{\bullet}] = 2[O_i^{''}] \quad (5)$$

However, this cannot be confirmed by the present data alone, owing to the difficulties described above in interpreting the electrical property results. For example, this type of compensation mechanism, when combined with the parent compound's Frenkel-type defect[27] reaction should lead to a slope of $+^1/_4$ in Figure 6, parts a and b. This, however, is not the case because of the narrow width of this "intrinsic" region with respect to oxygen partial pressure variations. Shallow slopes are observed instead, although their nonzero values indicate that the electron−hole pairs should be considered "minority" defect species. The easily accessible plane of structural oxygen vacancies (see Figure 1b) allows for an ionic compensation mechanism, and interstitial oxygen defects have been observed in other layered cuprates with the double, square-pyramidal copper layers, including materials with the quadruple perovskite structure.[22,31,48−50] The small band gaps, as presented in Table 1, further complicate the interpretation of these results because large populations of electrons and holes lead to competing electroneutrality effects, and a more general equation is most likely applicable:

$$p + [Nb_{Sn}^{\bullet}] = 2[O_i^{''}] + n \quad (6)$$

because the populations of electrons and holes (n and p) cannot truly be assumed to be negligible species (kT is on the order of the band gap energies). The increase in the slope of the curves in Figure 6, parts a and b, at low temperatures is in agreement with this model in that the electronic carriers play a less important role in the overall electroneutrality condition as the number of thermally generated carriers decreases. This indicates that the niobium-doped materials should be considered as oxygen-excess materials, $La_2Ba_2Cu_2Sn_{2-x}Nb_xO_{11+x/2\pm\delta}$ ($x/2$ represents the oxygen-content variation with doping and δ represents the ability to further alter the anionic composition by controlled-atmosphere annealing). While this model appears reasonable, further experiments are required to completely understand the defect mechanisms. With respect to attaining new superconductors, the lack of electronic compensation is the most important aspect that can be definitely ascertained from the present data. From a solid-state chemical point of view, the inability to stabilize appropriately oxidized or reduced materials adopting this structure-type represents an intriguing dilemma, which is fundamental to understanding the relationship of the inner architecture to the internal chemistry of layered copper oxides, as discussed below.

4. Discussion

The primary goal of this research was to use high-temperature electrical property measurements in combination with crystal chemical studies to understand which aspects of the inner architecture control the stability of carriers, particularly electrons, in the copper−oxygen networks of layered cuprates. We have presented the high-temperature (the near-synthesis temperature region) electrical properties of the quadruple perovskite $La_2Ba_2Cu_2Sn_{2-x}Nb_xO_{11+x/2\pm\delta}$ to understand the relationship of the long, in-plane copper−oxygen bond lengths to the redox behavior of layered copper oxides. In this section, these results will be compared to those of various prior investigations to illuminate some clear trends in layered copper oxides. Most importantly, the overall in-plane copper−oxygen bond length plays an important role in the stability of carriers in layered copper oxides, but cannot be considered as the sole factor.

That layered copper oxide structures can be built by stacking copper-based perovskite layers (often oxygen-deficient) with layers based on various other structural motifs, such as rock salt, fluorite, and perovskite, leads to mismatches between the equilibrium bond distances of the individual layers. As Goodenough and Manthiram[32] argue, residual internal stresses arising from interlayer mismatch stabilize particular oxidation states for the copper−oxygen network. For example in $Nd_{2-x}Ce_xCu_2O_4$,[32] the Nd_2O_2 fluorite layer places the CuO_2 square planes in tension, because of its larger size. Introduction of the smaller cerium in the fluorite layer and an electron in the CuO_2 layer both serve to reduce this internal strain. This is exactly what is observed in the high-temperature electrical properties, which are shown in Figure 7 (along with other related materials): cerium doping leads to a progressive reduction of the copper−oxygen network and to extrinsic, highly doped, n-type behavior and an appropriate electronic state for superconductivity. This behavior is in stark contrast to that observed in the niobium-doped quadruple perovskites presented herein. As implied by this argument, the starting point for the search of new n-type superconductors should begin with long bond length materials, thus favoring the addition of an electron into the antibonding Cu-$d_{x^2-y^2}$/O-2p manifold.

Considering the two known, layered perovskites containing copper and tin as the framework *B*-cations, both shown in Figure 1 and both having in-plane copper−oxygen bond lengths greater than 2 Å, it is intriguing that neither material is amenable to electron doping. The electrical properties of the quadruple per-

(46) Mason, T. O. In *Electronic Ceramic Materials*; Nowotny, J., Ed.; Trans Tech Publications: Zurich, 1992; pp 503−536.
(47) Schoonman, J. In *The CRC Handbook of Solid State Electrochemistry*; Gellings, P. J., Bouwmeester, H. J. M., Eds.; CRC Press: Boca Raton, 1997.
(48) Caignaert, V.; Nguyen, N.; Raveau, B. *Mater. Res. Bull.* **1990**, *25*, 199−204.
(49) Currie, D. B.; Weller, M. T.; Rowles, S.; Gregory, D. H. *Mater. Res. Bull.* **1990**, *25*, 1279−1286.
(50) Lightfoot, P.; Pei, S.; Jorgensen, J. D.; Tang, X.-X.; Manthiram, A.; Goodenough, J. B. *Physica C* **1990**, *169*, 464−468.

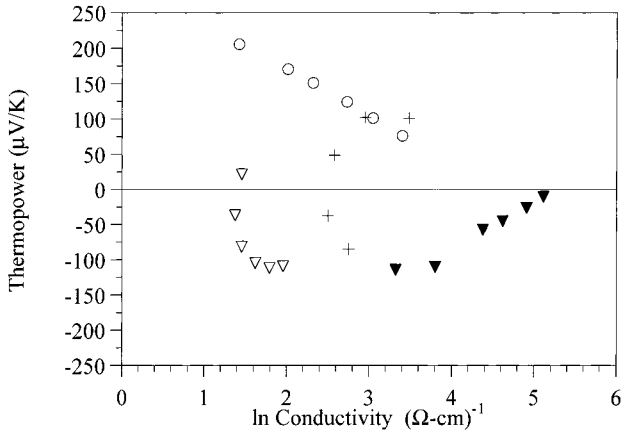

Figure 7. Jonker plots of (▽) $La_2Ba_2Cu_2Sn_{1.85}Nb_{0.15}O_{11}$; (○) $NdDyBa_{1.5}Sr_{0.15}Cu_{2.2}Ti_{1.8}O_{11}$, after ref 22; (+) $La_3Ba_3Cu_6O_{14\pm x}$, after ref 38; and (▲) $Nd_{2-x}Ce_xCuO_4$, after ref 41. All data from $T \approx 800$ °C. For the latter compound, values correspond to $x = 0.007$, 0.02, 0.05, 0.08, 0.10, and 0.15 in order of increasing conductivity. For the prior three compounds, data corresponds to various oxygen partial pressures as discussed for Figures 2−5.

ovskite discussed above demonstrate that a long, in-plane bond length is not a sufficient condition to favor the reduction of the CuO_2^{2-} planes. The internal stresses in this material might, at a first glance, be considered to be similar to those of $Nd_{2-x}Ce_xCuO_4$: the small copper-based perovskite double-layers are in tension because of their mismatch to the larger tin-based perovskite double layers. Following this argument, we expect that substitution of the smaller niobium for tin should therefore lead to electron doping, to alleviate these internal stresses. However, this is not experimentally observed (see Figure 7 for the difference between the two n-type, substituted systems) and will be shown to be, in fact, an incorrect view. Whatever the extent of the reduction that occurs in $La_2Ba_2Cu_2Sn_2O_{11}$ as a result of niobium substitution (as observed in Figures 3−5), which is dependent on the position of the intrinsic composition (n = p) with respect to temperature, oxygen partial pressure and niobium content, it is insufficient to lead to an electronic state appropriate for superconductivity, and is drastically different to that observed for $Nd_{2-x}Ce_xCuO_4$.

Similar arguments to those given above concerning the stability of n-type doping in cuprates can be made for La_2CuSnO_6 where the copper−oxygen bonds are in tension from the larger tin−oxygen networks. The high-temperature electrical properties of this series have been presented elsewhere.[30] Experimentally, it was observed that p-type doping was preferred in this system, achieved by strontium substitution for lanthanum, in complete disagreement with the simple picture of bond lengths discussed above. Moreover, in this system we observed that n-type substitutions are not stable, at least not with niobium substitution for tin in La_2CuSnO_6, which is a plausible chemical substitution, as evidenced in the $La_2Ba_2Cu_2Sn_{2-x}Nb_xO_{11+x/2\pm\delta}$ system. Prior investigations into the absence of superconductivity and the stability of holes in the $La_{2-x}Sr_xCuSnO_6$ system led to the proposal that the d_{z^2} orbitals play a prominent role in the electronic states near the Fermi level, in contrast to superconducting layered cuprates.[28−30] The distinct difference of this double perovskite to the high-T_c cuprates has been evidenced directly by the persistent antiferromagnetism[28] and relatively high p-type, thermopower values, despite extensive hole doping[30] (∼0.15 holes per copper cation). The competition of the d_{z^2} orbital, which is perpendicular to the CuO_2^{2-} layer, with the in-plane $d_{x^2-y^2}$ orbital demonstrates the importance of the coordination environment of copper in its redox capability. The long, in-plane bond lengths also play a cooperative role, leading to behavior markedly different from that of La_2CuO_4, which also contains octahedral copper but superconducts with a T_c near 40 K. Schematic band structures (adapted from ref 28), of the copper d orbitals, are given in Figure 8, parts a and b, to illustrate the fundamental difference between the superconducting La_2CuO_4 and nonsuperconducting La_2CuSnO_6.

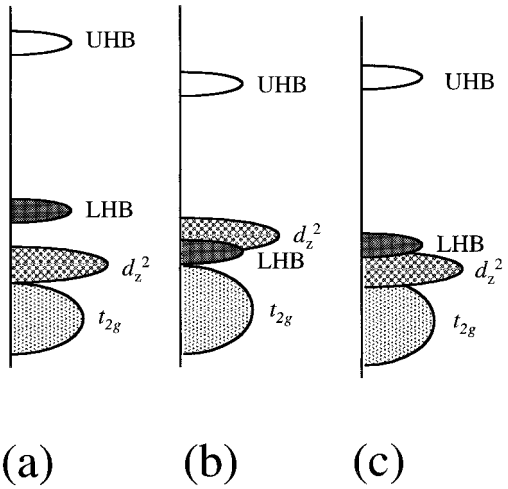

Figure 8. Schematic band structure diagram for the Cu d orbital region of (a) La_2CuO_4, (b) La_2CuSnO_6, and (c) $La_2Ba_2Cu_2Sn_2O_{11}$. The two-electron $d_{x^2-y^2}$ band is correlation split into a filled one-electron Lower Hubbard Band (LHB) and an empty one-electron Upper Hubbard Band (UHB). Parts a and b are adapted from ref 28, and part c is a schematic based on the logic presented herein.

In La_2CuSnO_6, the octahedral coordination of copper coupled to the structural distortions associated with the large blocking layer cation, maintain the antibonding d_{z^2} orbital at an energy level higher than the lower Hubbard band derived from the antibonding $d_{x^2-y^2}$ orbital (see Figure 8b). Recently, Ln_2CuSnO_6 (Ln = Pr, Nd, and Sm) and La_2CuZrO_6 have been stabilized using a high-pressure synthetic technique (6−8 GPa) and were found to adopt the ordered−layered structure of La_2CuSnO_6.[51] The high-pressure compounds were found to be antiferromagnets with a value of the exchange interaction (J) similar to the layered cuprates, i.e., La_2CuSnO_6 and Nd_2CuO_4. In these layered cuprates the magnetic interactions are dominated by the *filled*, one-electron, lower Hubbard band derived from the $d_{x^2-y^2}$ orbital which lies in the copper−oxygen plane. It is important to note that the Hubbard splitting of the half-filled, parent two-electron band can lead to a situation where the filled, lower Hubbard band drops to an energetic position below the d_{z^2} band.[28] Thus, two-dimensional antiferromagnetic interactions are not inconsistent with an electronic structure where the

(51) Azuma, M.; Kaimori, S.; Takano, M. *Chem. Mater.* **1998**, *10*, 3124−3130.

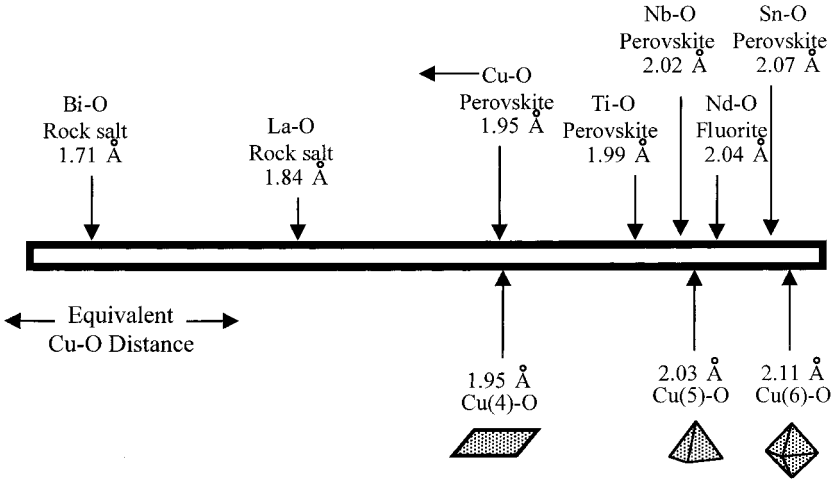

Figure 9. Estimated equilibrium bond distances of various structural components which comprise layered cuprates. Ionic radii are taken from ref 54 and the distances are those projected along the copper−oxygen bond length in the perovskite-based layer, shown on the lower half of the schematic.

valence band is derived from a different orbital, such as the d_{z^2} orbital (Figure 8). A comparison of plots of the reduced thermopower versus the natural logarithm of the conductivity for $La_{2-x}Sr_xCuSnO_6$ and $La_{2-x}Ba_xCuO_4$ reveals a fundamental difference in their electronic structure which is consistent with the idea that the doped holes are introduced into the d_{z^2} orbitals in the $La_{2-x}Sr_xCuSnO_6$ family of compounds.[30] The difference in the thermopower behavior with doping arises from the different density of states available to holes in a two-electron d_{z^2}-derived band or a one-electron, Hubbard-split $d_{x^2-y^2}$-derived band. The latter is, however, responsible for the magnetic behavior in *both* cases leading to similar magnetic behavior.

In order for superconductivity to be favored in the copper oxides, the $d_{x^2-y^2}$ orbital should retain its position closest to the Fermi level. This is true when the apical oxygen are removed from octahedrally coordinated copper, thereby lowering the energy of the d_{z^2} orbital. The extreme case of this stabilization is for square-planar geometry of the CuO_2^{2-} sheets, as in $Nd_{2-x}Ce_xCuO_4$ and $Sr_{1-x}Ln_xCuO_2$, which can be electron-doped sufficiently to observe superconductivity.[5,6] The intermediate case exists for the double square-pyramidal active layers, such as those in $La_2Ba_2Cu_2Sn_2O_{11}$, where a single apical oxygen has been removed (see schematic band structure in Figure 8c compared to Figure 8b). Both p-type and n-type behaviors are observed in these pyramidal copper compounds, depending on the in-plane bond length.[22−27,31] The amphoteric nature of the quadruple perovskite compounds, as observed in Figures 2−5, suggest that the $d_{x^2-y^2}$ orbital is the most closely associated with the Fermi level, as indicated in band structure calculations.[52,53] However, the observed asymmetry in the conduction parameters of the copper−stannate quadruple perovskite, which is unique among layered cuprates may be an indication of a more complex interaction of the copper and oxygen orbitals near the Fermi level. This possible complex interaction also inhibits useful speculation as to the origin of the asymmetry of the conduction parameters.

To assess correctly the relevant internal stresses in these layered materials, we must take into account the coordination environment of copper: which may be four-, five-, or six-coordinate in layered copper oxides. Using Shannon's ionic radii,[54] we can estimate the "equilibrium" copper−oxygen bond lengths for Cu^{2+} in each type of environment. These values are given on the lower half of the schematic in Figure 9. It must be emphasized that Shannons's ionic radii are spherically symmetric on the basis of empirical bond averages; therefore these may only approximate the highly anisotropic, d^9 Cu^{2+} Jahn−Teller cation. On the upper half of the schematic in Figure 9 are equilibrium bond distances, projected along the copper−oxygen bond direction, of several other important structural units which comprise layered cuprates. Thus it can be immediately seen that using Goodenough and Manthiram's arguments, for La_2CuO_4, combining octahedral Cu−O with rock salt La−O units, and for Nd_2CuO_4, containing square planar Cu−O with fluorite Nd−O units, the mismatches lead to hole and electron stabilization, respectively. Furthermore, Bi−O layers are extreme in their compressive mismatch and may explain the ease of overdoping these materials with holes. Adding four-coordinate copper layers to five-coordinate layers (as for $YBa_2Cu_3O_7$) also leads to compressive stresses on the five-coordinate copper layers. However, for tin−oxygen bonds, of 2.07 Å, there is very a small *tensile* stress for five-coordinate copper and a small compressive stress for the octahedral copper, in this scenario. In both cases, the residual stresses are small and, in fact, the two layers appear to be nearly matched with respect to their equilibrium lengths. Rotations of the tin−oxygen octahedra appear to absorb all of the mismatch in the $La_2Ba_2Cu_2Sn_2O_{11}$ compound.[15]

As mentioned above, the "equilibrium" bond lengths should be considered as estimates because the Cu^{2+} cation undergoes cooperative, static Jahn−Teller distortions (which polarizes the d_{z^2} cation in a direction normal to the layer). Thus, it would be interesting to empirically determine the equilibrium in-plane bond length for each type of coordination environment. This

(52) Mattheiss, L. F. *Phys. Rev. B* **1992**, *45*, 2442−2446.
(53) Novikov, D. L.; Freeman, A. J.; Poeppelmeier, K. R. *Phys. Rev. B* **1996**, *53*, 9448−9452.
(54) Shannon, R. D. *Acta Crystallogr.* **1976**, *A32*, 751−767.

is possible for the case of the square-pyramidal coordination because the $La_2Ba_2Cu_2Sn_2O_{11}$ material displays intrinsic (i.e., copper predominantly in the divalent state) behavior over a wide range of temperatures and oxygen partial pressure. This implies that the copper−oxygen bond length in this material, of 2.01 Å,[15] is approximately the equilibrium bond distance. It may also be noted that this is not far from the estimate given in Figure 9. If we compare the behavior of this material with the "equilibrium" bond length to related structures with smaller bond lengths, we expect slightly modified behavior.

This is precisely what is observed in the isostructural $Ln_2Ba_2Cu_2Ti_2O_{11}$ (Ln = lanthanide), wherein copper−oxygen bond lengths near 1.96 Å,[27] which are in compression with respect to the equilibrium distance, lead to a slight favoring of p-type carriers, even in unsubstituted materials. The triple perovskite, $LaBa_2Cu_2NbO_8$ has identical copper coordination and bond lengths near 1.99 Å,[7,9] and displays behavior between the two quadruple perovskites $La_2Ba_2Cu_2Sn_2O_{11}$ (Cu−O ≈ 2.01 Å) and $Ln_2Ba_2Cu_2Ti_2O_{11}$ (Cu−O ≈ 1.96 Å).[22,27,31] The data for the quadruple perovskite $NdDyBa_{1.5}Sr_{0.5}Cu_{2.2}Ti_{1.8}O_{11\pm\delta}$ (which has considerably smaller in-plane bond lengths, ≈ 1.95[22]) are given in Figure 7 to demonstrate that appropriate chemical alterations can indeed lead to extensive p-type behavior, particularly in reduced bond length materials. Thus we can conclude that the equilibrium distance is near 2.01 Å, and the instability of large concentrations of electrons in the $La_2Ba_2Cu_2Sn_{2-x}Nb_xO_{11}$ material is a result of bond matching between the layers and the lack of an internal stress as a driving force to favor reduction of the copper−oxygen sheets.

Furthermore, the ability of the structure to tolerate an extensive amount of oxygen intercalation in the plane of ordered oxygen vacancies between the copper−oxygen planes helps stabilize the incorporation of niobium. Similar substitution behavior was observed for the titanium-based quadruple perovskites, $Ln_2Ba_2Cu_2Ti_2O_{11}$ (Ln = lanthanide); extensive substitutions on each site of the structure (not including the copper site) are only possible if they are isovalent or ionically compensated. Substitutions which require a valence change of copper, in these nominally bond-matched layered copper oxides, were found to have extremely limited solid solution ranges. Similarly, niobium substitution of tin in La_2CuSnO_6 is not stable because there is no facile ionic compensation mechanism available in this close-packed structure. Whereas interstitial oxygen offset the similar substitution in the quadruple perovskite, there is no room in the double perovskite to tolerate interstitial oxygen and therefore the niobium substitution is unfavored. The nominal match between the six-coordinate tin and copper lends no driving force to the stabilization of electrons, when in fact it is already observed that holes are slightly favored as carriers in this material.

Considering the stabilization of electronic carriers from the bond-mismatch model perspective, coupled with the equilibrium bond length of various copper polyhedra, it is interesting to ask: (1) what types of materials would be stabilized as electron doped structures? And, (2) what type of superconductors might be stabilized from the quadruple and double perovskite structures? The two known n-type superconductors contain square-planar copper units—which have the smallest equilibrium bond lengths. Whether or not the absence of apical oxygen is a requirement for the observation of n-type superconductivity is an open question. To test this experimentally, one requires related structures with equivalent carrier concentrations and different copper coordinations. However, the present analysis indicates that facile electron doping, driven by the appropriate tensile stress state, will likely occur only in layered cuprates having five- or six-coordinate copper if the counter layer has an equilibrium distance (projected along the direction of the copper−oxygen bond) greater that 2.1−2.2 Å. Even if materials with this type of structure were realized, an unwanted stabilization of the d_{z^2} orbital with respect to the $d_{x^2-y^2}$ orbital, as observed in La_2CuSnO_6, is extremely likely. Thus, the lack of apical oxygen serves to reduce the in-plane equilibrium copper−oxygen bond length, to lower the energy of the d_{z^2} orbital away from the Fermi level, and to allow for the incorporation of layers with the appropriate mismatch to stabilize the synthesis of reduced materials. Therefore it is not suprising that there is a paucity of n-type cuprates from a synthetic chemistry point of view. Further research into possible n-type superconductivity in layered cuprates having five- and six-coordinate copper is warranted, but will require precise chemical control over the inner architecture of these materials in the synthesis stage.

With respect to the second question posed above, it appears that $La_2Ba_2Cu_2Sn_2O_{11}$ prefers the intrinsic regime and is therefore a difficult material to drive into the superconducting regime. However, if we compare the high-temperature electrical data of this compound to that of $La_{1.5}Ba_{1.5}Cu_3O_{7\pm x}$ ($La_3Ba_3Cu_6O_{14\pm x}$), as done in Figure 7, we observe that the Jonker pears are extremely similar in size and shape for the two materials[27] (although it should be pointed out that contributions from the chain-type layers in the latter compound inhibit a strict comparison of their electronic structures). Substitution of 0.5 La^{3+} by Ba^{2+} in $La_{1.5}Ba_{1.5}Cu_3O_{7\pm x}$, while maintaining an appropriate oxygen concentration, leads to p-type superconductivity in $LnBa_2Cu_3O_{7-x}$. Various substitutions, aimed at realizing p-type superconductivity, in the quadruple perovskite system have led to p-type metallic behavior in the $NdDyBa_2Cu_2Ti_2O_{11\pm x}$ system,[22] but solid solution limits inhibit further carrier doping and the observation of superconductivity. On the other hand, to achieve n-type superconductivity, it appears that aliovalent and isovalent substitutions which put the copper-based layers in tension and inhibit an ionic compensation mechanism are required.

With respect to the double perovskite, La_2CuSnO_6, electron doping may be stabilized via synthetic techniques which raise the energy of the $d_{x^2-y^2}$ orbital with respect to the d_{z^2} orbital, thereby changing the electronic structure of this material. One possible method would be to synthesize these materials under extreme pressure conditions, which could compress the copper−oxygen bonds. Azuma et al. synthesized several new compounds which adopt this layered-cuprate, double-perovskite structure using a high-pressure synthetic technique.[51] Unfortunately, these interesting new compounds did not

have decreased bond lengths as hoped for, but rather an increased buckling of the copper−oxygen layers. If one could realize an anisotropic compression in the copper−oxygen plane, then electrons may be stabilized in the upper Hubbard band. In any case, the synthesis of materials with the appropriate electronic and structural requirements for superconductivity will require precise chemical control over the inner architecture.

5. Conclusions

These investigations into the physical properties of nonsuperconducting layered cuprates with pure perovskite-based structures, closely related to known superconducting materials, have reinforced the importance of the paramount relationships between the inner architecture, internal chemistry, and physical properties of solid-state materials. We have presented the high-temperature electrical properties of $La_2Ba_2Cu_2Sn_{2-x}Nb_xO_{11+x/2\pm\delta}$ and demonstrated that electronic compensation is not favored for this substitution scheme under normal synthetic conditions. Rather, the niobium substitution is made possible by the incorporation of extra oxygen in the plane of ordered oxygen vacancies. A similar substitution in the oxygen-stoichiometric double-perovskite La_2CuSnO_6 is not possible because neither electronic compensation nor ionic compensation is energetically favorable owing to the lack of either internal stresses on the copper−oxygen layers or lattice sites to incorporate excess oxygen. Comparing various layered cuprates illustrates that interlayer stresses can be considered strong driving forces for the stabilization of electronic compensation, an essential requirement for the observation of superconductivity. Furthermore, the paucity of electron-doped cuprates is shown to be related to the difficult structural conditions required to favor electron stabilization in the $d_{x^2-y^2}$ orbital, while maintaining the d_{z^2} orbital at an energy removed from the Fermi level.

Acknowledgment. This work was supported by the National Science Foundation (Award No. DMR-91-20000) through the Science and Technology Center for Superconductivity and made use of MRL Central Facilities supported by the National Science Foundation, at the Materials Research Center of Northwestern University (Award No. DMR-9120521). The authors would like to thank S. J. Ford and J. W. Koenitzer for helpful discussions.

CM9811489